The Horizontal Diffusion of Tracers by Surface Waves

K. HERTERICH AND K. HASSELMANN

Max-Planck-Institut für Meteorologie, Hamburg, W. Germany

(Manuscript received 29 June 1981, in final form 21 January 1982)

ABSTRACT

The horizontal dispersion of tracers in the presence of a random field of ocean surface waves is examined. Random fluctuations in the local Stokes-drift current cause a water particle to follow a random-walk path. The associated diffusion coefficients for individual particles, particle pairs and a continuous tracer patch can be calculated rigorously within the framework of perturbation analysis. For a fully developed Pierson-Moskowitz wave spectrum all diffusion coefficients scale as the third power of the wind speed and are typically of the order 10^{-2} m^2 s^{-1} for a wind speed of 10 m s^{-1}. The diffusion coefficients are strongly anisotropic and decrease approximately exponentially with depth below the sea surface.

1. Physical mechanism of wave-induced dispersion

Observations of the horizontal dispersion of tracers in the upper layer of the ocean are usually interpreted in terms of eddy diffusion processes. A basic difficulty in modeling these processes is the broad range of scales of the natural eddy spectrum of the ocean, which normally makes it impossible to separate the space or time scales of the tracer distribution from the scales of the mixing eddies. Thus classical Fickian diffusion theories, which require that the scale of the mixing eddies be small compared to the scale of the tracer distribution, are not applicable. Models of the dispersion of tracers by oceanic turbulence have therefore largely been limited to semi-empirical scaling relations based on rather simple dimensional arguments (cf. Okubo, 1962).

Although horizontal eddies of approximately the same scale as the tracer distribution are probably responsible for mixing at scales larger than a few kilometers, there is some evidence that for smaller scales surface waves may yield an equally important contribution to horizontal dispersion. Diffusion measurements by Schott *et al.* (1978) indicate that the diffusion coefficients for these scales tend to increase with the surface-wave height. In the present paper we investigate this alternative mechanism theoretically and compute dispersion rates for typical surface-wave spectra. Our analysis supports the conjecture that surface waves can yield a significant contribution to dispersion for small scales of the order of decameters to a few kilometers.

In contrast to the problem of eddy diffusion, the dispersion of a scalar tracer by surface waves is a problem which can be closed statistically and treated rigorously by perturbation methods. This comes about because the autocorrelation time of the random velocity perturbations responsible for diffusion is small compared with the diffusion time scale, so that two-scale statistical techniques are applicable. The process may, in fact, be regarded as a particular case of a resonant interaction at zero frequency, as already pointed out by Hasselmann (1966, 1968).

The dispersion mechanism can be readily understood physically in terms of random fluctuations of the Stokes-drift current.

For a sinusoidal deep-water surface wave the mean Lagrangian (Stokes) drift current, obtained by expanding the potential-flow wave solution to second order, is given by

$$\mathbf{u}_s(z) = 2\omega\mathbf{k}\overline{\zeta^2}e^{2kz}, \tag{1.1}$$

where $\overline{\zeta^2}$ is the mean-square surface displacement, $\omega = (gk)^{1/2}$ and k are the frequency and wavenumber of the waves, g is the gravitational acceleration, and z is the vertical coordinate, measured positive upwards from the mean surface. More generally, for a random field of ocean surface waves, the ensemble-mean Stokes-drift is given by the sum of the contributions (1.1) from all individual components of the wave spectrum

$$\langle \mathbf{u}_s(z) \rangle = 2 \iint F(\mathbf{k})\omega\mathbf{k}e^{2kz}d\mathbf{k}, \tag{1.2}$$

where the spectrum is defined here as the variance spectrum of the surface displacement $\iint F(\mathbf{k})d\mathbf{k} = \overline{\zeta^2}$.

Computations of the Stokes-drift (1.2) for typical wave spectra have been made by Bye (1967), Kenyon (1969) and Chang (1969). For a fully developed Pierson-Moskowitz (1964) spectrum, for which the peak frequency scales as the inverse wind speed U

0022-3670/82/070704-08$06.00

and the mean-square wave height as the fourth power of U, Eq. (1.2) yields

$$u_s(z = 0) = a \cdot U,$$

with $a \approx 0.013$ (U is defined here as the wind speed at 10 m anemometer height). A Stokes-drift current of this order represents a significant contribution to the total wind drift at the sea surface, which is estimated from measurements to be of the order of 2–3% of the wind speed.

The Stokes-drift velocity represents the average velocity of a particle at a given depth, for an averaging time large compared with the wave period. Over shorter periods, however, individual particles will experience drift-velocity fluctuations relative to the mean value due to the statistical fluctuations of the local wave amplitudes in a random sea. If the wave field is regarded as a random superposition of statistically independent wave packets, each of which is associated with its own Stokes-drift velocity, a fluid particle experiencing the passage of a sequence of wave packets will be exposed to a fluctuating drift current, in analogy to the Brownian motion of a particle exposed to random external forces. Thus any given water particle at a given location experiences a local second-order velocity, whose mean value is given by the mean Stokes-drift (1.2), but which fluctuates about this mean. From the Rayleigh statistics of the amplitudes of wave groups it follows that the fluctuations u'_s will generally be of the same order as the mean u_s (note that we refer here to fluctuations of the second-order Lagrangian velocities, not to the larger, first-order orbital velocities of higher frequency which, as shown below, do not contribute to the diffusion process). From random-walk theory it is known that such random velocity fluctuations result generally in a particle dispersion which, for large dispersion times, can be represented as a Fickian diffusion process. The diffusion coefficient is given by

$$D = \langle u'^2_s \rangle \tau, \tag{1.3}$$

where $u'_s = u_s - \langle u_s \rangle$ is the local deviation of the second-order Lagrangian drift velocity relative to its mean value $\langle u_s \rangle$ (= Stokes-drift) and τ represents the (one-sided) integral autocorrelation time of the fluctuations.

According to (1.3) [cf. also (2.3) and (2.3′)], Fickian diffusion by random continuous motion occurs only if the integral of the Lagrangian velocity autocorrelation function exists and is non-zero. In the frequency domain, this is equivalent to the condition that the variance spectrum of the Lagrangian velocities at zero frequency is finite and non-zero. In the formal second-order perturbation analysis presented in Section 2 it will be shown that this condition is indeed satisfied for the second-order Lagrangian velocity field (the spectral density for the first-order, finite-wavelength, linear wave field is, of course, zero at zero frequency).

Using Eq. (1.3) an order of magnitude estimate of the diffusion coefficient may be obtained. For a random wave field characterized by a narrow spectrum of bandwidth $\Delta\omega$, $\tau \sim (\Delta\omega)^{-1}$ and from the Rayleigh statistics of wave-group amplitudes $\langle u'^2_s \rangle \sim \langle u_s \rangle^2$. Taking $\langle u_s \rangle \approx 0.1 - 0.2$ m s^{-1}, $\Delta\omega \approx 1 - 0.4$ s^{-1}, one obtains $D \approx 0.01 - 0.1$ m^2 s^{-1}. This is comparable with the orders of magnitude of Fickian diffusion coefficients estimated from tracer-patch dispersion experiments for small time and space scales in the range $T \sim$ O (1 h), $L \sim$ O (30–3000 m) (cf. Schott *et al.*, 1978).

For wave-induced diffusion, the autocorrelation time scales of the horizontal velocity fluctuations are generally small compared with the horizontal tracer-dispersion times of interest. Thus a Fickian diffusion description of the dispersion process is applicable. For single-particle diffusion relative to a reference frame moving with the mean drift velocity (which is appropriate, for example, for an ensemble of independent single-buoy drift experiments), the diffusion coefficient is independent of scale. However, if relative particle displacements are considered (tracer or buoy-cluster experiments) the diffusion coefficient becomes independent of scale only when the horizontal-distribution scale becomes large compared with the extent of the wave groups. In both cases, however, the inequality of the autocorrelation and dispersion time scales ensures the applicability of the Fickian diffusion formalism.

2. Mathematical derivation

Before considering the statistical fluctuations experienced by a particle in a random surface-wave field, we recall first the basic results of the classical theory of diffusion by random continuous motion (cf. Einstein, 1905; Taylor, 1921).

A particle whose velocity $u_i(t)$ ($i = 1, 2, 3$) undergoes statistically stationary fluctuations generally follows a random-walk path $x_i(t)$ which is characterized by non-stationary statistics. For large times t, both the mean and variance of x_i increase linearly with time:

$$\langle x_i \rangle = \langle u_i \rangle t, \tag{2.1}$$

$$\langle (x_i - \langle x_i \rangle)(x_j - \langle x_j \rangle) \rangle = 2D_{ij}t, \tag{2.2}$$

where

$$D_{ij} = \frac{1}{2} \int_{-\infty}^{\infty} R_{ij}(\tau) d\tau \tag{2.3}$$

$$= \pi G_{ij}(0) \tag{2.3′}$$

and

$$R_{ij}(\tau) = \langle u'_i(t + \tau) u'_j(t) \rangle, \tag{2.4}$$

$$G_{ij}(\omega) = \frac{1}{2\pi} \int_{-\infty}^{\infty} R_{ij}(\tau) e^{-i\omega\tau} d\tau, \tag{2.5}$$

represent, respectively, the covariance function and cross-spectrum of the particle-velocity fluctuations $u_i' = u_i - \langle u_i \rangle$. The angle brackets denote averages over an infinite ensemble of particles associated with different realisations of the velocity function but the same initial value $x_i = 0$ for $t = 0$.

Eqs. (2.1), (2.2) hold asymptotically for times t which are large compared with the integral covariance time scales

$$\tau_{ij} = \int_{-\infty}^{\infty} R_{ij}(\tau)d\tau / R_{ij}(0) = 2\pi G_{ij}(0) \Big/ \int_{-\infty}^{\infty} G_{ij}(\omega)d\omega.$$

If Eqs. (2.1), (2.2) are applied to an ensemble of particles characterized by a continuous concentration function $c(\mathbf{x}, t)$, the rate of change of c is given by the advective-diffusive equation

$$\frac{\partial c}{\partial t} + \frac{\partial}{\partial x_i}(\hat{u}_i c) = \frac{\partial}{\partial x_i}\left(D_{ij}\frac{\partial c}{\partial x_j}\right), \qquad (2.6)$$

where

$$\hat{u}_i = \langle u_i \rangle - \frac{\partial D_{ij}}{\partial x_j}.$$

Eq. (2.6) also applies asymptotically under the two-scaling conditions $L \gg (D\tau)^{1/2}$, $T \gg \tau$, where L, T represent the characteristic space and time scales of the distribution c, while D, τ denote the orders of magnitude of D_{ij} and τ_{ij}. Under these conditions the statistical properties of the velocity field, and therefore also the mean quantities $\langle u_i \rangle$, D_{ij}, can be regarded as slowly varying functions of $\mathbf{x}$ and t.

The dispersion of particles in a quasi-homogeneous, quasi-stationary random surface-wave field clearly represents a particular case of the general theory of diffusion by continuous motion. The present problem therefore reduces to the derivation of the mean advection velocity $\langle u_i \rangle$ and diffusion tensor D_{ij} for the velocity field associated with a random surface-wave field. The mean advection velocity is, of course, simply the well-known Stokes-drift current. However, the diffusion tensor D_{ij} has not been evaluated previously. The general structure of the term was discussed briefly by Hasselmann (1968) as one of a general set of weak-interaction processes in a surface-wave field. In this representation the diffusion process was regarded as a resonant interaction process for the particular case of a zero resonance frequency. Following this approach, we shall use the spectral expression (2.3′) for D_{ij} rather than the more familiar correlation integral (2.3). To keep the algebra simple we restrict ourselves to an infinite-depth ocean (which is a good approximation for ocean depths larger than about one-fourth of the wavelength).

A random surface-wave field may be regarded in the linear approximation as a superposition of an ensemble of statistically independent, normally distributed wave components

$$\zeta = \sum_{\mathbf{k}} [Z_{\mathbf{k}}^{+} e^{i(\mathbf{k}\cdot\mathbf{x} - \omega t)} + Z_{\mathbf{k}}^{-} e^{-i(\mathbf{k}\cdot\mathbf{x} - \omega t)}], \qquad (2.7)$$

where

$$Z_k^{-} = (Z_k^{+})^*,$$

$$\langle Z_{\mathbf{k}_1}^{s_1}(Z_{\mathbf{k}_2}^{s_2})^* \rangle = \tfrac{1}{2}\delta_{\mathbf{k}_1\mathbf{k}_2}\delta_{s_1 s_2}F(\mathbf{k}_1)\Delta\mathbf{k}_1 . \qquad (2.8)$$

In Eq. (2.8), the asterisk denotes the complex conjugate, s_1, s_2 are sign indices, and $\Delta\mathbf{k}_1$ represents the (infinitely small) wavenumber increment of the sum (2.7).

For ocean waves, the nonlinearities of the waves are small, and the general nonlinear wave field (assuming irrotational, inviscid flow) can be constructed formally by a perturbation expansion with respect to the wave amplitudes (cf. Phillips, 1960; Hasselmann, 1961; Longuet-Higgins, 1962; and others),

$$\begin{Bmatrix} v_i \\ w \end{Bmatrix} = \sum_{\mathbf{k},s} \begin{Bmatrix} V_{i\mathbf{k}}^{s} \\ W_{\mathbf{k}}^{s} \end{Bmatrix} Z_{\mathbf{k}}^{s} \exp\{i\cdot s(\mathbf{k}\cdot\mathbf{x} - \omega t) + kz\}$$

$$+ \sum_{\substack{\mathbf{k}_1,s_1 \\ \mathbf{k}_2,s_2}} \begin{Bmatrix} V_{i\mathbf{k}_1\mathbf{k}_2}^{s_1 s_2} \\ W_{\mathbf{k}_1\mathbf{k}_2}^{s_1 s_2} \end{Bmatrix} \exp\{i[(s_1\mathbf{k}_1 + s_2\mathbf{k}_2)\mathbf{x}$$

$$- (s_1\omega_1 + s_2\omega_2)t] + (k_1 + k_2)z\}, \qquad (2.9)$$

where v_i $(i = 1, 2)$ and w denote the horizontal and vertical components of the velocity field, and the linear coefficients are given by

$$\left.\begin{aligned} V_{i\mathbf{k}}^{s} &= k_i/k\omega \\ W_{\mathbf{k}}^{s} &= -is\omega \end{aligned}\right\}. \qquad (2.10)$$

The nonlinear coupling coefficients are given in the references cited. For the following, however, we require only the result that the quadratic coupling coefficients vanish for $\omega_1 = \omega_2$ and $s_1 = -s_2$. For this reason the nonlinear terms in (2.9) do not contribute to the mean second-order (Eulerian) velocity and, as shown below, also do not contribute to particle diffusion (to the lowest, quadratic order).

For the dispersion of particles the Eulerian velocities (v_i, w) at fixed positions are of less concern than the Lagrangian velocities of individual particles, which have a non-vanishing mean equal to the Stokes drift. The Lagrangian vertical drift and diffusion terms are found to vanish (as expected on the basis of the heuristic explanation of the diffusion process given in Section 1), so that we need consider in the following only the horizontal velocity components u_i. These can be expressed to lowest, quadratic order in terms of the corresponding Eulerian components by expanding with respect to the orbital displacements,

$$u_i(\mathbf{x}, z) = v_i(\mathbf{x} + \boldsymbol{\xi}, z + \zeta)$$

$$= v_i(\mathbf{x}, z) + \frac{\partial v_i}{\partial x_j}\xi_j + \frac{\partial v_i}{\partial z}\zeta, \qquad (2.11)$$

where $\mathbf{x}$, z denote the mean position of a particle, averaged over a wave period, and $\xi = (\xi_1, \xi_2, \zeta)$ is the instantaneous displacement of the particle relative to this position. Substituting the expansion (2.9) into (2.11) we obtain

$$u_i = \sum_{\mathbf{k},s} V^s_{i\mathbf{k}} Z^s_{\mathbf{k}} \exp[is(\mathbf{kx} - \omega t) + kz] + \sum_{\substack{\mathbf{k}_1,\mathbf{k}_2 \\ s_1,s_2}} U^{s_1 s_2}_{i\mathbf{k}_1\mathbf{k}_2} Z^{s_1}_{\mathbf{k}_1} Z^{s_2}_{\mathbf{k}_2} \exp\{i[(s_1\mathbf{k}_1 + s_2\mathbf{k}_2)\mathbf{x} - (s_1\omega_1 + s_2\omega_2)t] + (k_1 + k_2)z\}, \quad (2.12)$$

where

$$U^{s_1 s_2}_{i\mathbf{k}_1\mathbf{k}_2} = \frac{\omega_1 k_{1_i} + \omega_2 k_{2_i}}{2k_1 k_2} \times (k_1 k_2 - s_1 s_2(\mathbf{k}_1\mathbf{k}_2)) + V^{s_1 s_2}_{i\mathbf{k}_1\mathbf{k}_2}. \quad (2.13)$$

The expectation value of (2.12) yields Eq. (1.2) for the mean Stokes drift $\langle u_i \rangle$. To obtain the diffusion coefficient D_{ij} we need to determine the cross spectral density matrix G_{ij} at zero frequency [Eq. (2.3′)]. Invoking the Gaussian property of the Fourier components $Z_{\mathbf{k}}{}^s$ and assuming that the first-order spectrum $F(\mathbf{k})$ is zero at $\mathbf{k} = 0$, so that the linear terms do not contribute to the zero-frequency energy density, one obtains from (2.12)

$$D_{ij} = \pi G_{ij}(0) = \pi \int \cdots \int T_{ij}(\mathbf{k}_1, \mathbf{k}_2) F(\mathbf{k}_1) F(\mathbf{k}_2) \times \delta(\omega_1 - \omega_2) d\mathbf{k}_1 d\mathbf{k}_2, \quad (2.14)$$

with

$$T_{ij}(\mathbf{k}_1, \mathbf{k}_2)_{(\omega_1=\omega_2)} \cdot = (U^{+-}_{i\mathbf{k}_1\mathbf{k}_2} U^{-+}_{j\mathbf{k}_1\mathbf{k}_2})_{(\omega_1=\omega_2)} = \frac{\omega^2}{4}\left(1 + \frac{\mathbf{k}_1 \cdot \mathbf{k}_2}{k^2}\right)^2 \times (k_{1i}k_{2j} + k_{2i}k_{1j} + k_{1i}k_{1j} + k_{2i}k_{2j}), \quad (2.15)$$

where $\omega = \omega_1 = \omega_2$, $k = k_1 = k_2$.

The δ-function is most easily eliminated in (2.14) by transforming to frequency-directional spectra, $F(\mathbf{k})d\mathbf{k} = F(\omega, \theta)d\omega d\theta$. Eq. (2.14) then becomes

$$D_{ij} = \pi \iiint T_{ij} F(\omega, \theta_1) F(\omega, \theta_2) d\omega d\theta_1 d\theta_2. \quad (2.16)$$

The diffusion-coefficient tensor D_{ij} is constant for a given wave spectrum and characterizes the dispersion of an ensemble of particles relative to a reference point moving with the mean Stokes velocity.

In many applications it is also useful to consider diffusion tensors defined with respect to relative displacements of particles. The simplest case is the relative dispersion of two particles a, b which are separated initially by the distance $r_i = x_i^a - x_i^b$. Assuming both particles to be at the same depth, the mean separation rate vanishes, $\langle dr_i/dt \rangle = \langle u_i^a \rangle - \langle u_i^b \rangle = 0$. The two-particle diffusion tensor $\tilde{D}_{ij} = \langle (r_i - \langle r_i \rangle)(r_j - \langle r_j \rangle) \rangle / 2t$ is calculated in exactly the same way as for the single particle case, except that the nonlinear coupling coefficient for the relative velocity now becomes

$$\tilde{U}^{s_1 s_2}_{i\mathbf{k}_1\mathbf{k}_2} = U^{s_1 s_2}_{i\mathbf{k}_1\mathbf{k}_2}(1 - \exp[i(s_1\mathbf{k}_1 + s_2\mathbf{k}_2)\mathbf{r}]). \quad (2.17)$$

The diffusion coefficient $\tilde{D}_{ij}$ characterizing the rate of relative dispersion of pairs of particles is accordingly given by Eq. (2.16), but with the kernel T_{ij} replaced by

$$\tilde{T}_{ij} = 2T_{ij}\{1 - \cos[(\mathbf{k}_1 - \mathbf{k}_2) \cdot \mathbf{r}]\}. \quad (2.18)$$

For small $\mathbf{r}$, $\tilde{T}_{ij} \to 0$, as expected, since the two particles experience essentially the same velocity fluctuations, whereas for large $\mathbf{r}$, $\tilde{T}_{ij} \to 2T_{ij}$, in accordance with the standard relation for two particles dispersing independently.

The Fickian diffusion equation (2.6) is also applicable to pair dispersion, the probability density referring in this case to the distribution of displacements for an ensemble of pairs of particles. The particle-pair diffusion equation is useful for interpreting experiments with clusters of drifter buoys. In such experiments the reference point for single-particle diffusion, which moves with the (ensemble) mean Stokes-drift velocity, is not always well defined by the finite buoy cluster. A dispersion formulation in terms of pair separations avoids this difficulty. In addition, particle-pair separation data are more abundant than single-particle data: a cluster of n buoys yields only n displacement values relative to the mean, while the same cluster yields $n(n-1)/2$ relative separation values.

However, in situations in which individual particle marking is not feasible, for example in tracer-patch experiments, one has no recourse other than to consider the dispersion relative to the mean drift. Since the ensemble-mean Stokes-drift cannot be determined from a finite-size tracer patch, the appropriate reference velocity must be defined by the motion of the center of gravity of the tracer patch itself.

The modifications of the single particle relations (2.12)–(2.16) required to treat this case are again minor. Defining an instantaneous mean position and velocity of the tracer patch (at a given depth) by

$$\tilde{x}_i = \iint x_i c(\mathbf{x}) d\mathbf{x},$$

$$\tilde{u}_i = \iint u_i c(\mathbf{x}) d\mathbf{x},$$

where $c(\mathbf{x})$ is the (normalized) tracer concentration, the instantaneous velocity of a particle at a position $\mathbf{x}$ relative to the mean patch velocity is again given by (2.12), but with a modified linear term (which is irrelevant, since the linear term does not contribute

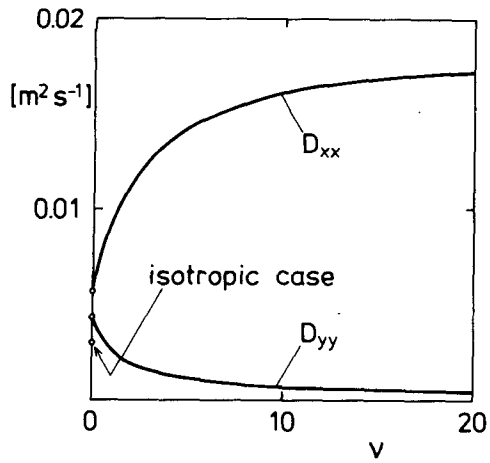

FIG. 1. Principal components D_{xx} and D_{yy} of the diffusion tensor for single-particle diffusion for different exponents ν of the angular spreading function $S(\theta) \propto \cos^{\nu}(\theta)$ [cf. Eq. (3.7)].

to the diffusion or mean drift) and a modified nonlinear coefficient

$$\hat{U}^{s_1 s_2}_{i\mathbf{k}_1\mathbf{k}_2} = U^{s_1 s_2}_{i\mathbf{k}_1\mathbf{k}_2}\Big\{1 - \int\int \exp[i(s_1\mathbf{k}_1 + s_2\mathbf{k}_2) \times (\mathbf{x}' - \mathbf{x})]\ c(\mathbf{x}')d\mathbf{x}'\Big\}. \quad (2.19)$$

The diffusion coefficient $\hat{D}_{ij}$ is accordingly given by (2.16), as before, but with the kernel T_{ij} replaced by

$$\hat{T}_{ij} = T_{ij}\{1 + \mathrm{cm}^2 + \mathrm{sm}^2 - 2\,\mathrm{cm}\cdot\cos[(\mathbf{k}_1 - \mathbf{k}_2)\cdot\mathbf{x}] - 2\,\mathrm{sm}\cdot\sin[(\mathbf{k}_1 - \mathbf{k}_2)\cdot\mathbf{x}]\}, \quad (2.20)$$

where

$$\begin{Bmatrix}\mathrm{cm}\\ \mathrm{sm}\end{Bmatrix} = \int\int c(\mathbf{x}')\cdot\begin{Bmatrix}\cos[(\mathbf{k}_1 - \mathbf{k}_2)\cdot\mathbf{x}']\\ \sin[(\mathbf{k}_1 - \mathbf{k}_2)\cdot\mathbf{x}']\end{Bmatrix}d\mathbf{x}'. \quad (2.21)$$

The diffusion coefficient $\hat{D}_{ij}$ depends both on the particle position $\mathbf{x}$ relative to the patch center $\bar{\mathbf{x}}$ and on the size of the patch. Although Eqs. (2.20), (2.21) are independent of the choice of origin, it is convenient to place the origin of the x_1, x_2 plane at the center of the patch. For small patches, it is then seen that cm $\to$ 1, sm $\to$ 0, and Eq. (2.20) takes the form (2.18) corresponding to two-particle diffusion. For large patches, cm $\to$ 0, sm $\to$ 0, and one recovers the single-particle relation (2.15). Thus the tracer-patch diffusion problem may be regarded as an intermediate case between the single-particle and particle-pair dispersion cases.

3. Numerical calculations

Examples of the diffusion tensors D_{ij} were calculated from the integral (2.16) for the cases of single, pair and patch diffusion. For simplicity the wave spectrum F was assumed separable into a one-dimensional frequency spectrum $f(\omega)$ and a frequency-independent directional spreading factor $S(\theta)$,

$$F(\omega, \theta) = f(\omega)\cdot S(\theta), \quad (3.1)$$

where $S(\theta)$ is normalized such that

$$\int_{-\pi}^{\pi} S(\theta)d\theta = 1.$$

The one-dimensional spectra were taken as Pierson-Moskowitz or JONSWAP spectra of the form

$$f(\omega) = \alpha g^2\omega^{-5}\psi(\omega/\omega_m)\exp\left[-\frac{5}{4}\left(\frac{\omega_m}{\omega}\right)^4\right], \quad (3.2)$$

where ω_m denotes the peak frequency, α is Phillips's constant and $\psi(\omega/\omega_m)$ is a shape function which describes the enhancement of the peak of a fetch-limited JONSWAP spectrum relative to the fully-developed Pierson-Moskowitz spectrum.

For the Pierson-Moskowitz spectrum, the shape factor $\psi \equiv 1$, $\alpha = 0.0081$ and the peak frequency is determined by the wind speed U (at 19.5-m height above sea surface) through the relation

$$\omega_m = 0.140\cdot 2\pi g/U. \quad (3.3)$$

For the JONSWAP spectrum, the shape factor ψ has a maximal value $\psi(1) \approx 3.3$ at the peak, and α and ω_m vary with the state of development of the wind-sea.

For a spectrum of the general form (3.2) it follows from dimensional analysis of (2.16) that in all three diffusion cases the diffusion coefficients scale as

$$D_{ij} = \alpha^2 g^4\omega_m^{-3}\tilde{D}_{ij}, \quad (3.4)$$

where $\tilde{D}_{ij}$ is a nondimensional coefficient which depends only on the properties of the nondimensional shape functions $\psi(\omega/\omega_m)$ and $S(\theta)$.

For a fully developed Pierson-Moskowitz spectrum, Eqs. (3.3) and (3.4) imply

$$D_{ij} = 1.47\alpha^2 g U^3\tilde{D}_{ij}. \quad (3.5)$$

Most of the following examples are computed for a Pierson-Moskowitz spectrum with $U = 10$ m s^{-1}. The transformation to other wind speeds can be readily effected using (3.5). For single particle diffusion we obtain from (2.14), (2.15) and (3.1)

$$\begin{pmatrix}D_{xx} & D_{xy}\\ D_{yx} & D_{yy}\end{pmatrix} = \frac{\pi}{4g^2}\int_0^{\infty} d\omega\omega^6 f^2(\omega)\int_{-\pi}^{\pi} d\theta_1 S(\theta_1)\int_{-\pi}^{\pi} d\theta_2 S(\theta_2)[1 + \cos(\theta_1 - \theta_2)]^2 \times\begin{pmatrix}(\cos\theta_1 + \cos\theta_2)^2, & (\cos\theta_1 + \cos\theta_2)(\sin\theta_1 + \sin\theta_2)\\ (\cos\theta_1 + \cos\theta_2)(\sin\theta_1 + \sin\theta_2), & (\sin\theta_2 + \sin\theta_2)^2\end{pmatrix}. \quad (3.6)$$

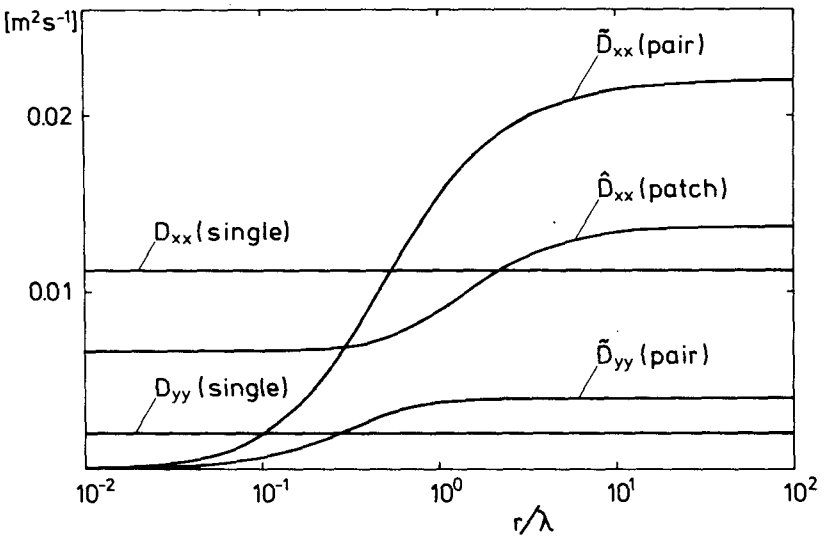

FIG. 2. Components D_{xx} of the diffusion tensor for single-particle, particle-pair and patch diffusion, and D_{yy} for single-particle and particle-pair diffusion as functions of r/λ = (diffusion scale/peak wave length) (cf. definitions given in text and Fig. 3).

For a symmetrical spreading function $S(\theta)$ about the wind direction $\theta = 0$, which we define as the x-axis, the non-diagonal components $D_{xy} = D_{yx}$ vanish. Fig. 1 shows the components D_{xx} and D_{yy} for a Pierson-Moskowitz spectrum at $U = 10$ m s^{-1} as a function of the narrowness of the spreading function, as characterized by the exponent ν in the spreading function representations

$$S(\theta) = \begin{cases} A_\nu \cos^\nu(\theta); & |\theta| < \dfrac{\pi}{2} \\ 0; & \dfrac{\pi}{2} \leqslant |\theta| < \pi \end{cases}, \qquad (3.7)$$

where A_ν denotes a normalization factor.

Also shown is the isotropic case, $S(\theta) = 1/2\pi$ plotted at $\nu = 0$, although it should be noted that the limit $\nu \to 0$ of (3.7) corresponds in fact to the half-plane and not to the full-plane isotropic case). As expected, narrower directional distributions yield more pronounced diffusion in the x-direction than in the y-direction.

For particle pair diffusion, T_{ij}, Eq. (2.16), must be replaced by $\tilde{T}_{ij}$ from (2.18). This introduces the additional factor

$$2\{1 - \cos[(\mathbf{k}_1 - \mathbf{k}_2)\cdot\mathbf{r}]\}$$
$$= 2\left(1 - \cos\left\{\frac{\omega^2}{g} r[\cos(\theta_1 - \beta) - \cos(\theta_2 - \beta)]\right\}\right),$$

into the integrand of (3.6), where β denotes the angle between the x-axis and the vector separation $\mathbf{r}$ between the two particles. Because of this factor, the integration variables ω and θ_1, θ_2 can no longer be separated.

The corresponding diffusion tensor $\tilde{D}_{ij}$ is now in general a function of $\mathbf{r}$. The computations for $\tilde{D}_{xx}$ and $\tilde{D}_{yy}$ are shown in Fig. 2. The vector separation $\mathbf{r}$ is taken parallel to the x-axis, the mean wave direction, and is scaled in units of λ, the peak wavenumber of the Pierson-Moskowitz spectrum (3.2). A $\cos^2\theta$ angular distribution is used for $S(\theta)$ [Eq. (3.7) with $\nu = 2$]. Also shown for comparison is the constant single-particle diffusion coefficient D_{ij}, which is equal to half the asymptotic value ($r \to \infty$) of the particle-pair diffusion coefficient $\tilde{D}_{ij}$.

Finally, patch diffusion coefficients were computed for an isotropic and normalized Gaussian tracer concentration

$$c(\mathbf{x}) \propto \exp[-(2|\mathbf{x}|/\lambda)^2]$$

with a horizontal scale given by λ, centered at the origin of the coordinate system ($\tilde{\mathbf{x}} = 0$). With this choice of scale the patch is neither sufficiently small for the patch to move simply as a single particle [particle-pair diffusion limit: cm $\to$ 1, sm $\to$ 0 (see Section 2)], nor sufficiently large for the center of mass of the patch to stay essentially at the same place (single-particle diffusion limit: cm $\to$ 0, sm $\to$ 0). This is borne out by the curve for the patch diffusion coefficient $\hat{D}_{ij}$ shown in Fig. 2: the limiting values at $r/\lambda = 0$ and for $r/\lambda \to \infty$ are seen to differ from the corresponding values for both single-particle and particle-pair diffusion. Note that the abscissa variable r/λ represents in the case of the patch diffusion coefficient the dimensionless distance of a given particle from the center of the patch. The geometry and nomenclature for the three diffusion cases presented in Fig. 2 are summarized in Fig. 3.

The relatively small transverse diffusion coeffi-

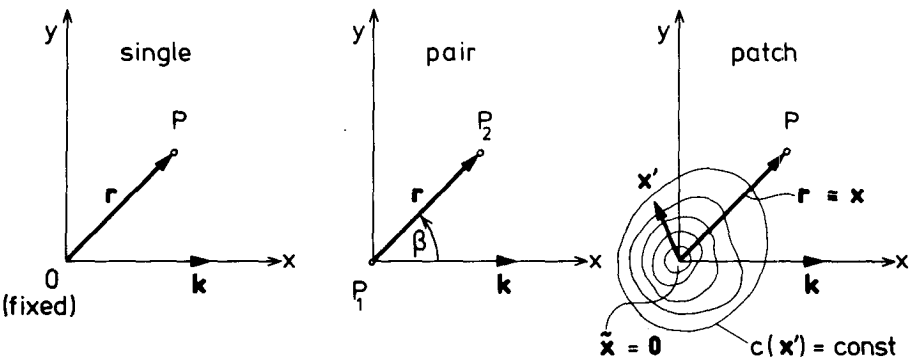

FIG. 3. Geometry and notation for single-particle, particle-pair and patch diffusion.

cients D_{yy} are shown in Fig. 2 only for the cases of single-particle and particle-pair diffusion. It may be noted that for particle-pair diffusion $\tilde{D}_{yy}$ approaches its asymptotic value for $r \to \infty$ more rapidly than $\tilde{D}_{xx}$. This is due to the fact that a Pierson-Moskowitz spectrum with a $\cos^2\theta$ angular spreading function is broader (in the neighborhood of the peak) in the cross-wind k_y-direction than in the downwind k_x-direction, so that the correlation length is smaller in the y-direction than in the x-direction.

Nondiagonal contributions to the diffusion tensor arise if $S(\theta)$ is nonsymmetrical and also, in the case of pair diffusion, if $\mathbf{r}$ is not parallel to the mean wave direction $\mathbf{k}$. Fig. 4 shows the dependence of $\tilde{D}_{ij}$ for the latter case on β, the angle between $\mathbf{r}$ and $\mathbf{k}$, for the value $r/\lambda = 1$ for which the β dependence is most pronounced. (For $r = 0$ and $r \to \infty$ the diffusion tensor $\tilde{D}_{ij}$ becomes independent of β [see Eq. (2.18)].

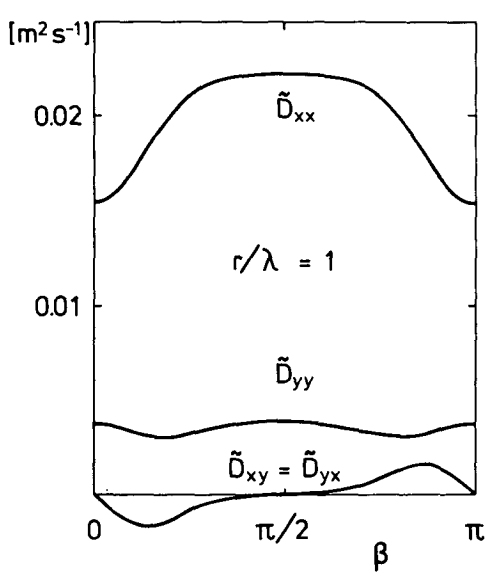

FIG. 4. The three components $\tilde{D}_{xx}$, $\tilde{D}_{yy}$ and $\tilde{D}_{xy} = \tilde{D}_{yx}$ of the diffusion tensor for particle-pair diffusion for $r/\lambda = 1$ as a function of β, the angle between the vector distance $\mathbf{r}$ between the two particles and the x-axis (the mean wind direction).

The maximum in $\tilde{D}_{xx}$ at $\beta = \pi/2$ is again due to the smaller correlation length of the wave spectrum in the y-direction.

In addition to the results shown here for a Pierson-Moskowitz spectrum a number of computations were also made for a JONSWAP spectrum, which is more appropriate for a growing wind-sea than the fully developed Pierson-Moskowitz spectrum (Hasselmann *et al.*, 1973). For a given wind speed, the diffusion coefficients for a fetch-limited JONSWAP spectrum are smaller than for a Pierson-Moskowitz spectrum, essentially because the fetch-limited spectrum contains less energy than the fully developed spectrum.

To conclude this section, it should be pointed out again that all results presented here apply for a medium wind speed $U = 10$ m s^{-1}. Since the diffusion coefficients scale as the third power of U [Eq. (3.5)], considerably higher values are obtained for higher wind speeds.

4. Comparison with measurements

Although a random surface wave field will necessarily produce dispersion, it is not yet clear whether the process can compete with other horizontal diffusive processes in the upper layer of the ocean, such as eddy turbulence.

Diffusion experiments in the ocean have been made on a variety of space and time scales. Few, however, have been combined with sufficiently detailed wave measurements to determine how much of the observed diffusion may have been due to waves. Okubo (1971) has compared a large number of diffusion experiments from different investigations and finds a mean scale dependence of the diffusion coefficients for all experiments proportional to $L^{1.1}$, where L is the space scale of the diffusing patch. Although the definitions of diffusion coefficient and space scale used by Okubo and in this paper are somewhat different, we may nonetheless compare the orders of magnitude of the theoretical wave-induced diffusion with these measurements. From Fig. 5, taken from Okubo (1971), it may be inferred that for scales

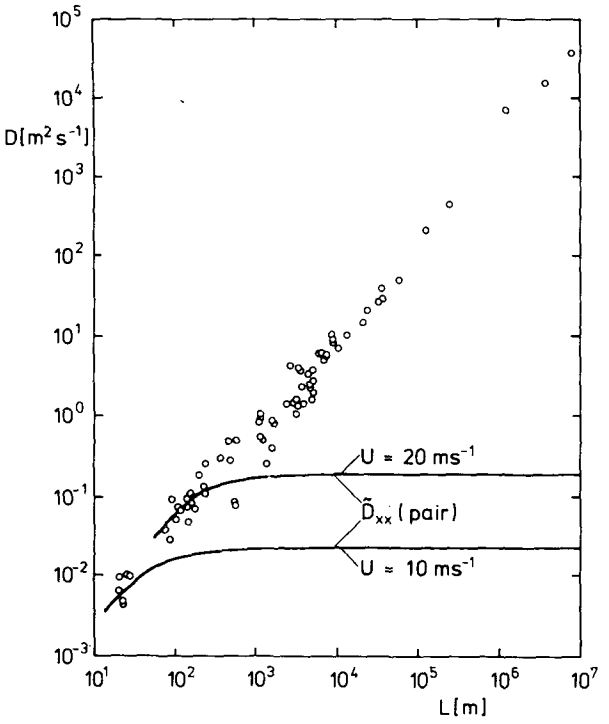

FIG. 5. Comparison of measured diffusion coefficients (from Obuko, 1971) with wave-induced (particle-pair) diffusion as a function of scale.

larger than ~1 km, the contribution due to wave-induced diffusion will generally be negligible, but for scales between 10 and 100 m, wave diffusion may be an important contributing mechanism.

However, to clarify this question, more detailed dispersion experiments in the space–time scale range of 10–10^3 m, 0.1–10 h, supported by wave measurements, are needed. Several characteristic features of wave-induced diffusion can aid in identifying wave-induced diffusion in the presence of other diffusion mechanisms. The process is strongly anisotropic, with considerably larger diffusion rates in the mean propagation direction of the waves than in the transverse direction. Also, the strength of the diffusion decreases rapidly with the depth d below the surface. The rate of decrease is approximately proportional to e^{-4kd}, where k is the peak wavenumber of the wave spectrum. Thus for a Pierson-Moskowitz spectrum with a wind speed of $U = 10$ m s^{-1} the diffusion coefficient is already reduced to $1/e$ of the surface value at a depth of only 3 m. This property is, of course, only relevant for float dispersion experiments. Horizontal dye diffusion in a vertically mixed layer is governed by the vertically averaged horizontal diffusion coefficient and is also affected by the vertical shear of the mean Stokes-drift via the coupling of vertical diffusion and vertical mean shear (cf. Kullenberg, 1972). The diffusion process, finally, is strongly wind-speed dependent. Increasing the wind speed U not only increases the strength of the diffusion coefficient as U^3, but also increases the scale L characterizing the asymptotic transition of the pair-diffusion coefficient to its limiting value (twice the single-particle value) in accordance with the relation $L \propto U^2$ [cf. Eq. (3.3) and Fig. 5].

A general assessment of the significance of wave-induced diffusion relative to other diffusion processes in a given situation will require, of course, not only a knowledge of the local wave field, but also an understanding of the parameters controlling turbulent and other non-wave-diffusion processes. Unfortunately, this is still a largely unsolved problem. However, it may be encouraging that at least one of the processes contributing to horizontal diffusion in the ocean is amenable to a quantitative analysis, and that the process may indeed play an important role in the small scale: initial diffusion of concentrated injections into the ocean, such as occur in practice through oil spills, or the dumping of chemical contaminants.

REFERENCES

Bye, J. A. T., 1967: The wave drift current. *J. Mar. Res.*, **25,** 95–102.

Chang, M.-S., 1969: Mass transport in deep-water long-crested random gravity waves. *J. Geophys. Res.*, **74,** 1515–1536.

Einstein, A., 1905: Ueber die von der molekular-kinetischen Theorie der Waerme geforderte Bewegung von in ruhenden Fluessigkeiten suspendierten Teilchen. *Ann. Phys.*, **4,** 549–560.

Hasselmann, K., 1961: On the non-linear energy transfer in a gravity wave spectrum. Part 1: General theory. *J. Fluid Mech.*, **12,** 481–500.

——, 1966: Feynman diagrams and interaction rules of wave–wave scattering processes. *Rev. Geophys.*, **4,** 1–32.

——, 1968: Weak interaction theory of ocean waves. *Basic Developments in Fluid Dynamics*, Vol. 2, M. Holt, Ed., Academic Press, 117–182.

——, et al., 1973: Measurements of wind wave growth and swell decay during the Joint North Sea Wave Project (JONSWAP). *Deutsch. Hydrogr. Z.*, Ergaenzungsheft, Reihe A, **8,** No. 12, 95 pp.

Kenyon, K. E., 1969: Stokes drift for random gravity waves. *J. Geophys. Res.*, **74,** 6991–6994.

Kullenberg, G., 1972: Apparent horizontal diffusion in stratified vertical shear flow. *Tellus*, **24,** 17–28.

Longuet-Higgins, M. S., 1962: Resonant interactions between two trains of gravity waves. *J. Fluid. Mech.*, **12,** 321–332.

Okubo, A., 1962: A review of theoretical models for turbulent diffusion in the sea. *J. Oceanogr. Soc. Japan*, **20,** 286–320.

——, 1971: Oceanic diffusion diagrams. *Deep-Sea Res.*, **18,** 789–802.

Phillips, O. M., 1960: On the dynamics of unsteady gravity waves of finite amplitude, 1, The elementary interactions. *J. Fluid. Mech.*, **9,** 193–217.

Pierson, W. J., and L. Moskowitz, 1964: A proposed spectral form for fully developed wind seas based on the similarity theory of S. A. Kitaigorodskii. *J. Geophys. Res.*, **69,** 5181–5190.

Schott, F., M. Ehlers, L. Hubrich and D. Quadfasel, 1978: Small scale diffusion experiments in the Baltic surface-mixed layer under different weather conditions. *Dtsch. Hydrogr. Z.*, **31,** 195–215.

Taylor, G. I., 1921: Diffusion by continuous movements. *Proc. London Math. Soc.*, **20,** 196–211.